

# UWBCarGraz Dataset Measurement Report

Jakob Möderl, Stefan Posch, Franz Pernkopf and Klaus Witrisal  
Graz University of Technology (jakob.moederl@tugraz.at)

## I. OVERVIEW

This document contains an overview of the measurement setup, data processing and measurement protocol for the ultra-wideband (UWB) car occupancy detection measurement campaign carried out at Graz University of Technology in September 2022. If the dataset is used in any capacity, please cite the dataset as [1] or the corresponding paper [2].

## II. MEASUREMENT SETUP

The main goal of the measurement campaign is to develop and evaluate algorithms to detect car occupants using UWB radar. We performed measurements to gather channel impulse responses (CIRs) between a transmit and receive antenna over time while a person was inside the car performing various activities. For the measurement an UWB maximum length-sequence (MLS) correlative channel sounder from Imsens [3] was used, which is based on the principle of correlative channel sounding [4]. A binary sequence with suitable autocorrelation properties (a large peak-to-off-peak ratio) is transmitted over the channel. At the receiver, the CIR is recovered using a correlation with the known code sequence. This MLS radar has one transmitter and two receiver ports. To utilize two different pairs of antennas in a monostatic setup as well as a bistatic radar setup between the pairs of antennas, the transmitter was multiplexed with a  $2 \times 1$  high-frequency switch from minicircuits. The transmit power of the MLS device in FCC mode is 18 dBm. The employed 12-bit MLS has a length of 4095 samples. At the clock rate of 6.95 GHz, this allows for a maximum delay of  $\tau_{\max} = 589.2$  ns, which corresponds to a frequency resolution of  $\Delta_f = 1/\tau_{\max} = 1.709$  MHz. The 6.95 GHz signal is mixed up with an intermediate frequency, such that it occupies the spectrum from 3.8 GHz - 10.2 GHz.

The transmitted signal was radiated from custom made antennas using Euro-cent coins [5, Figure B.5b]. Those antennas have an approximately uniform radiation pattern in the azimuth domain and zeroes at  $\pm 90^\circ$  elevation. Pairs of antennas were mounted in the passenger cabin of the cars under the roof near the A-pillar and B-pillar, respectively. The antennas in the pairs were oriented such that the zeros in the azimuth domain pointed towards each other to reduce the mutual coupling as much as possible. Figure 1 illustrates the measurement setup.

During the measurement, the car was parked in an underground parking garage with the heck of the car oriented towards the wall. The environment outside the car was static during the measurements. The measurement equipment was placed outside the car on a neighbouring parking spot. The doors and windows of the car were closed during measurement, except for a small slit in the drivers window, which was left slightly open to leave room for the cables to the antennas. A picture of the antenna placements inside the car as well as the environment in the vicinity of the car can be seen in Figure 2a–2b.

This research was partly funded by the Austrian Research Promotion Agency (FFG) within the project SEAMAL Front (project number: 880598). Furthermore, the financial support by the Christian Doppler Research Association, the Austrian Federal Ministry for Digital and Economic Affairs and the National Foundation for Research, Technology and Development is gratefully acknowledged.

All authors are associated with Graz University of Technology. Stefan Posch and Klaus Witrisal are further associated with the Christian Doppler Laboratory for Location-aware Electronic Systems.

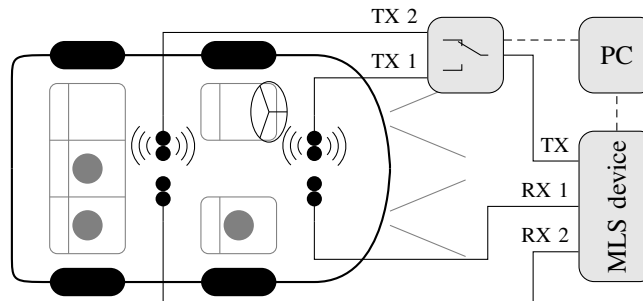


Fig. 1: Illustration of the measurement setup. The participant positions (front, back, middle) are indicated with gray circles.



Fig. 2: Antenna placement inside the Citroen Picasso (a) and the environment around the car (b).

### III. MEASUREMENT PROCESSING

Figure 3 shows a block diagram of the measurement setup. The system should be calibrated including the cables up to but not including the antennas. Hence, the influence of the device internal frequency responses and the frequency responses of the measurement cables and connectors combined in  $H_{\text{sys},1}(f)$  and  $H_{\text{sys},2}(f)$  as well as the crosstalk frequency responses between the TX channel and both RX channels  $H_{\text{cross},1}(f)$ ,  $H_{\text{cross},2}(f)$ , have to be compensated for both positions of the TX switch. For sake of brevity, we will drop the channel index 2. To measure these transfer functions, we performed two types of measurements. First, we terminated the output with a  $50\ \Omega$  match to measure the crosstalk frequency responses  $H_{\text{cross}}(f)$ . Second, also the RX antennas are unmounted and the TX and RX cables are connected. Hence, the measured frequency response is  $H_{\text{meas}}(f) = H_{\text{cross}}(f) + H_{\text{sys}}(f)$ . For capturing data, both the RX and TX antenna are mounted. Hence the measured frequency response over the full bandwidth of the measurement system is  $H_{\text{meas}}(f) = H_{\text{full}}(f)H_{\text{sys}}(f) + H_{\text{cross}}(f)$ . We obtain a calibrated version of the radio channels frequency response as

$$H_{\text{full}}(f) = \frac{H_{\text{meas}}(f) - H_{\text{cross}}(f)}{H_{\text{sys}}(f) - H_{\text{cross}}(f)}. \quad (1)$$

To avoid excessive noise gain, we use a thresholding on the time-domain representation of the denominator in (1) and set samples below the threshold to zero. The channels frequency response  $H(f)$  as seen by a practical radar system transmitting some baseband pulse  $S(f)$  at carrier frequency  $f_c$  over the channel is obtained by multiplying the full bandwidth frequency response  $H_{\text{full}}(f)$  with the pulse shape  $S(f)$  and compensating any time shift  $\tau_{\text{shift}}$  not already contained in  $H_{\text{sys}}(f)$ , such as the delay induced by the connectors and antennas, as

$$H(f) = H_{\text{full}}(f)S(f - f_c)e^{-j2\pi f\tau_{\text{shift}}}. \quad (2)$$

Finally, the time-domain CIR  $h(\tau)$  is obtained as the inverse Fourier transform of  $H(f)$ .

The dataset is available in two variants: (i) once with a raised cosine pulse as  $S(f)$  with a center frequency of  $f_c = 6.5$  GHz, a bandwidth of 500 MHz and a roll-off factor of  $\beta = 0.5$  corresponding to the UWB channel 5 in [6], and (ii) with a sinc-pulse as  $S(f)$  (i.e. a rectangular window in frequency domain) with a bandwidth of 5 GHz centered around  $f_c = 7$  GHz. The second version is intended for analysis or pre-processing with other pulses  $S(f)$  e.g. with different pulse shapes or center frequencies. Note, that the carrier frequency of the measurement system is at  $f_c = 6.95$  GHz. Due to the suppression of the carrier wave, the sensitivity of the measurement equipment is low at this frequency resulting in a high noise gain.

### IV. MEASUREMENT PROTOCOL

This section describes the measurement procedure for each volunteer. Each volunteer was measured individually and each volunteer was assigned an identification number to pseudonymize the data. Before the measurements, the volunteers were informed about the types of measurements which are being performed and signed a consent form. Each volunteer was asked to enter their age, weight and height in a list. During the measurement, each volunteer was assigned a position either in the front or back row of the car on the passenger side, or in the back row middle seat, and fitted with a belt that measured the expansion of the chest [7]. It was confirmed, that the belt was placed firmly but still comfortably around the chest of the volunteer. Next, they were instructed to sit in the car and remain as still as possible while continuing to breath as usual. Once the volunteers

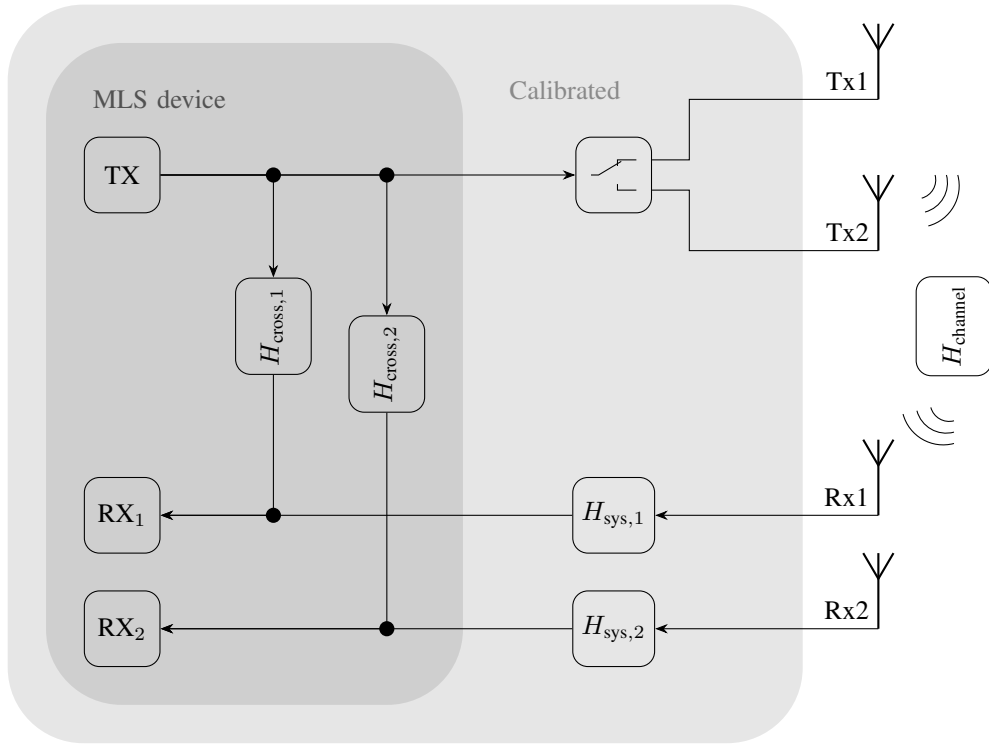


Fig. 3: For calibration, the channels  $H_{\text{cross},1}$ ,  $H_{\text{cross},2}$ ,  $H_{\text{sys},1}$  and  $H_{\text{sys},2}$  were measured for both positions of the switch.

TABLE I: Bio-metrics of the volunteers.

	min	max	median	unit
height	158	190	178.5	cm
weight	45	158	72	kg
age	22	64	29	years

were settled, approximately 2 minutes of CIRs were recorded at intervals of  $T_{\text{st}} = 0.1$  s. After the first measurement, the volunteers were instructed to continuously speak for a duration of 2 minutes for the next measurement. The volunteers were given the choice of either improvising a monologue on their own or reading from a book provided to them. Again, CIRs were recorded for approximately two minutes. Finally, for the last measurement, the volunteers were instructed to search for small pieces of chocolate candies hidden inside the car. However, the volunteers were also asked to not crawl around inside the car or otherwise leave their assigned seat.

After the third and final measurements was finished, the volunteers were thanked for participating in the measurement campaign and the respiration belt was removed. The volunteers were informed that they can keep the chocolate candies they found as small appreciation gift for participating. Appendix A list the bio-metrics of the volunteers as well as their assigned position within each car.

## V. UWBCARGRAZ DATASET DESCRIPTION

The measurement campaign consisted of 34 adult volunteers (6 female, 28 male). Measurements have been performed with two different cars: a hatchback compact car (Car 1, Seat Leon) and a minivan (Car 2, Citroën C4 Picasso). Out of the 34 volunteers, 9 were recorded twice, once in each car, while the remaining 25 volunteers were recorded only in one of the cars for a total of 21 volunteers in the hatchback compact car and 22 volunteers in the minivan. Additionally, 5 minutes of data have been obtained from Car 2 while it was empty. Table I list the min, max and median of the volunteers height, weight and age. It is evident from Table I, that a diverse group participated in the measurement campaign. Table II lists the number of samples in the dataset for each of the cases and each car. A full overview of the bio-metrics and seating position of each volunteer can be found Appendix A.

Examples of the time-varying part of the received signal  $\tilde{\mathbf{R}}$  of the three different activity levels as well as for the empty car are shown in Figure 4. In the breathing case (i), the columns of  $\tilde{\mathbf{R}}$  have approximately the shape of a line-of-sight component followed by a dense multipath profile. The magnitude of each column changes according to the periodic chest movement of the target. In the talking case (ii), the chest motion is not periodic anymore and variations can be observed across different propagation delays. The maximum amplitude of the variations in the CIR ( $\approx 55$  dB) is larger compared to the breathing case

TABLE II: Number of Samples in the UWBCarGraz dataset.

	Car 1 (Seat Leon)			Car 2 (Citroën C4 Picasso)		
	Train	Val.	Test	Train	Val.	Test
Breathing	368	144	0	0	409	150
Talking	367	145	0	0	406	150
Moving	380	161	0	0	410	150
Empty	0	0	0	66	100	20

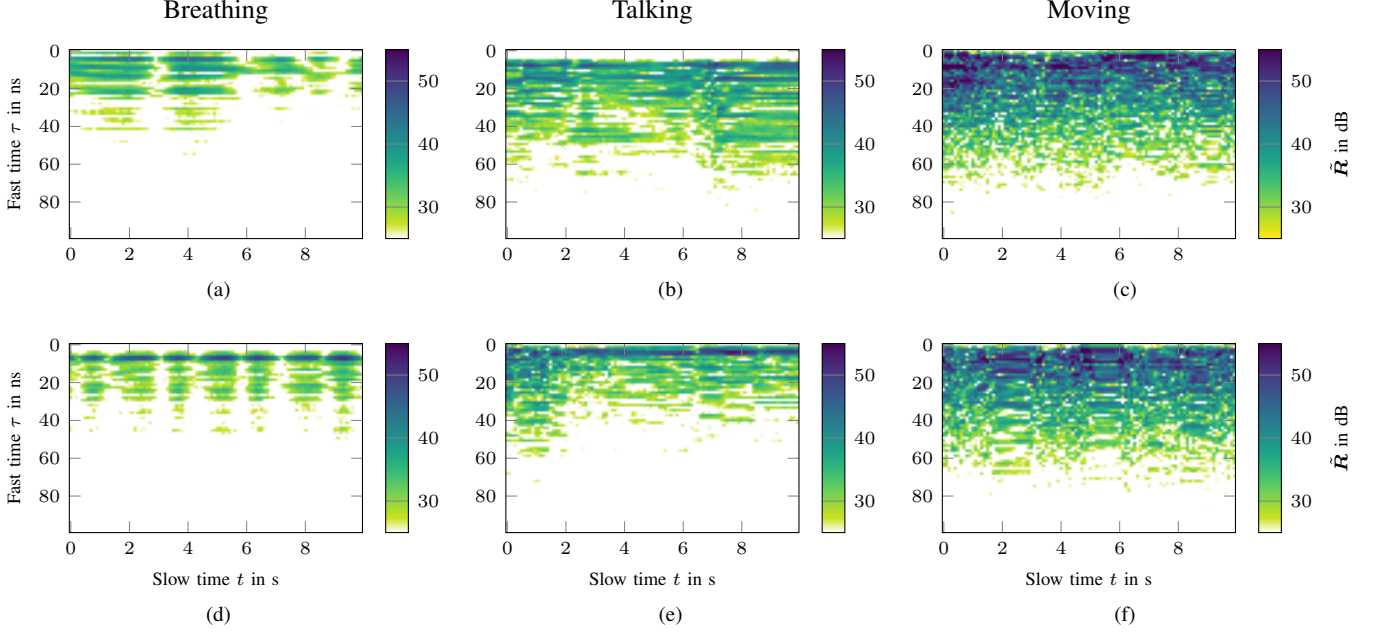


Fig. 4: Example signals from the dataset. The plots show the magnitude of the received signal  $\tilde{R}$  in dB for the breathing activity (a, d), talking activity (b, e) and moving activity (c, f). The x-axis is the measurement time in seconds (“slow time”) whereas the y-axis is the propagation delay in nanoseconds (“fast time”). Note, that the color scale is clipped so that all values  $\geq 55$  dB map to dark blue.

( $\approx 50$  dB). In the movement case (iii), no clear structure is visible in the data and the maximum amplitude of the variations ( $\approx 65$  dB) is once again larger compared to the talking case. Note, that the colorscale in Figure 4 is clipped such that all values  $\geq 55$  dB map to dark blue.

## APPENDIX

### A. Volunteer Info

Table III lists the seating position, transmit antenna and bio-metrics of each volunteer. If a seating position is denoted for both cars, the respective volunteer participated two times (once in each car), otherwise the respective volunteer participated only once.

## REFERENCES

- [1] J. Möderl, S. Posch, F. Pernkopf, and K. Witrals, “UWBCarGraz dataset,” Graz University of Technology, Nov. 2023, doi: <https://doi.org/10.3217/2gx2m-pt043>.
- [2] —, “UWBCarGraz dataset for car occupancy detection using ultra-wideband radar,” *ArXiv e-prints*, Nov. 2023. [Online]. Available: <https://arxiv.org/abs/2311.10478>
- [3] ILMSENS. m:explore - datasheet. Accessed: Oct. 2023. [Online]. Available: <https://www.ilmsens.com/app/download/14567836924/SH-3100%20-%20mexplore%20datasheet%2020170728.pdf>
- [4] A. F. Molisch, *Wireless Communications*, 2nd ed. Hoboken, NJ, USA: Wiley, 2011.
- [5] C. Krall, “Signal processing for ultra wideband transceivers,” PhD Thesis, Signal Process. and Speech Commun. Lab., Graz Univ. of Technol., Graz, Austria, 2008.
- [6] *IEEE Standard for Low-Rate Wireless Networks*, IEEE Std. 802.15.4-2020, Jul. 2020, (Revision of IEEE Std 802.15.4-2015).
- [7] Vernier Science Education, *Datasheet for Go Direct Respiration Belt*, accessed: Sep. 2023. [Online]. Available: <https://www.vernier.com/files/manuals/gdx-rb/gdx-rb.pdf>

TABLE III: Volunteer positions and bio-metrics.

ID	Sex	Bio-metrics			Seat Leon		Citroën Picasso	
		Weight (kg)	Height (cm)	Age (years)	Position	Active TX	Position	Active TX
01	m	71	173	26	Front	TX 1	Middle	TX 2
02	m	73	190	28	Back	TX 2	Front	TX 1
03	m	70	172	30	Front	TX 1	Back	TX 2
04	m	66	167	32	Back	TX 2	Middle	TX 2
05	f	45	158	26	Front	TX 1		
06	f	90	163	64	Back	TX 2	Back	TX 2
07	f	52	165	28	Front	TX 1		
08	m	158	176	31	Back	TX 2	Front	TX 1
09	m	78	178	32	Back	TX 1	Middle	TX 2
10	f	70	175	25	Front	TX 1		
11	m	71	176	32	Back	TX 2	Front	TX1
12	m	70	183	31	Front	TX 1		
13	m	77	175	28	Back	TX 1		
14	m	52	178	27	Front	TX 1		
15	m	130	178	33	Back	TX 2	Back	TX 2
16	m	89	183	30	Front	TX 1		
17	m	80	181	25	Back	TX 2		
18	m	95	183	28	Front	TX 1		
19	m	71	180	23	Back	TX 2		
20	f	56	163	27	Front	TX 1		
21	m	86	181	28	Back	TX 2	Back	TX 2
22	m	64	185	49				
23	m	67	181	30			Front	TX 1
24	m	67	181	30			Back	TX 2
25	m	72	173	28			Front	TX1
26	m	99	180	47			Front	TX 1
27	m	82	190	30			Middle	TX 2
28	m	74	181	37			Front	TX 1
29	m	72	168	33			Back	TX 2
30	m	63	168	48			Middle	TX 2
31	m	83	185	54			Front	TX 1
32	f	53	167	24			Back	TX 2
33	m	72	180	24			Front	TX 1
34	m	84	179	23			Back	TX 2